COMPARISON OF BROMINATED AND HALOGEN FREE FLAME RETARDANT BEHAVIOURS IN GLASS-FIBRE-REINFORCED POLY(BUTYLENE TEREPHTHALATE)

M. Suzanne*, J. Zhang*, S. Ukleja*, A. Ramani*, M.A. Delichatsios*, P. Patel, S. Shaw**, P. Clarke**, P. Cusack**,**
m.suzanne@ulster.ac.uk
*FireSERT, University of Ulster at Jordanstown, Shore Road, Newtownabbey, BT37 0QB, Northern Ireland
** ITRI, Unit 3, Curo Park, Frogmore, St. Albans, Hertfordshire, AL2 2DD, UK

Abstract
In this work, 30 wt. % glass fibre reinforced poly(butylene terephthalate), PBT, was modified with brominated polystyrene combined with antimony trioxide or aluminium diethylphosphinate (Alpi) with/without organically modified Montmorillonite clay (Nano-MMT). The efficiency of these fire retardants (FRs) was investigated in the cone calorimeter in both horizontal and vertical orientations by measuring, at six different heat fluxes, key flammability parameters such as time to ignition, heat release rate (HRR), smoke carbon monoxide and carbon dioxide yields and efficiency of combustion. All formulations exhibit charring burning behaviour having two peaks in the mass loss rate (MLR) and HRR because they leave a residue while pyrolysing consisting of glass fibres and char and/or nanoparticles. Compared to the base formulation, (PBT-GF), brominated polystyrene does not reduce the MLR but reduces significantly the HRR because bromine released in the pyrolysis gases inhibits combustion producing excessive carbon monoxide and smoke. Alpi alone has limited effect on the reduction of both MLR and HRR but, when combined with Nano-MMT, a significant reduction occurs of MLR and HRR without an increase in CO and smoke. The decrease in mass loss rate is due to the improved consistency of the residue (glass fibre, nanoparticles and char) produced by Alpi in the presence of nano-MMT whereas the reduction in the HRR is due directly to the reduction in the MLR because the measured heat of combustion is close to the heat of combustion of the basic formulation. Burning behaviour in horizontal or vertical orientations is similar except that lower HRRs are measured in vertical orientation owing to reduced flame heat fluxes compared to the burning in horizontal orientation. No dripping was observed in vertical orientation for all formulations. In addition, LOI and UL94 results for these materials are compared with the key flammability parameters in the cone calorimeter.

Introduction
In the past few years, the environmental and toxicological hazards of brominated flame retardants (BFRs) have been highlighted by several studies. It was demonstrated in [1-5] that for some of the BFRs results in a strong bioaccumulation in aquatic and terrestrial food chains, and a growing number of BFRs is found in increasing concentrations in the human food chain, human tissues and breast milk. Furthermore, BFRs have also been found in indoor environment such as in dust at homes [6]. BFRs are very persistent and show serious toxicological effects such as endocrine disruption. Brain and nervous system were identified as one of the most vulnerable targets for the toxic actions PBDE's [7]. It is therefore not surprising that some of the BFRs are or will be soon phased out. Consequently it is essential, for ecological and economical reasons, to investigate available environmental friendly alternatives. However, banning specific BFRs may imply a serious risk if the introduction of

non-brominated alternatives is not properly assessed regarding environment and human health. It is also important that substitution options do not affect the functionality and reliability of the end products and the fire behaviour is one of these aspects. This paper presents an evaluation of alternatives of brominated polystyrene in glass-fibre-reinforced poly(butylene terephthalate) (PBT-GF) for its fire retardancy. Other environmental aspects are being studied within the ENFIRO Project.

Materials

Four formulations listed in Table 1 are investigated in this study. The base formulation, PG1, consists of PBT reinforced with 30 wt. % of glass fibres. A halogenated formulation, PG2, contains 10 wt. % brominated polystyrene, with 5 wt. % antimony trioxide to seek a synergism effect. Two halogen free flame retardants (HFFRs) are studied: PG4A contains 15 wt. % aluminium diethylphosphinate (Alpi) and PG3B contains 15.5 wt. % Alpi combined with 2.5 wt. % nano-montmorillonite (Nano-MMT).

The virgin polymer and fire retardants were dried prior to extruding at 120°C under vacuum in an oven for 6 hours. A Prism Twin Screw Extruder (TSE) 16 TC was used to process the samples. The temperatures corresponding to the front zone, centre zone and rear zone were 255°C, 245°C and 240°C, respectively and the screw speed was set at 60 rpm. The extruded polymer was then pelletised and dried, as above. A BOY 22M was utilised to injection mould the samples. The temperatures corresponding to the rear zone, centre zone, front zone and nozzle zone were 240°C, 250°C, 250°C, and 260°C, respectively. These temperatures were varied by ± 5°C depending on the level for fire retardant present. The melt temperature was 255°C and the water-cooled mould was set at 80°C. The thickness of the samples is 2.9mm with a surface area of 0.1 x 0.1 m^2.

Table 1. Examined PBT-GF formulations.

Compounds	% weight of formulations				Commercial product name and suppliers
	PG1	PG2	PG3B	PG4A	
PBT-GF30	100	85	82	85	Arnite TV4 261 from DSM
Brominated polystyrene	0	10	0	0	Milebrome 7010 from MPI Chemie
Antimony trioxide	0	5	0	0	Timonox Red Star from Chemtura
Alpi	0	0	15.5	15	Exolit OP 1230 from Clariant
Nano-MMT	0	0	2.5	0	Cloisite 30B from Southern Clay Products

UL94 and LOI Tests

Prior to the cone calorimeter tests, LOI measurements and UL94 vertical tests were conducted using 3.2mm thick samples, according to BS EN 60695-11-10 and BS EN ISO 4589-2 respectively. The results are summarised in Table 2. The three FR-containing formulations are V0 rated while PG1 formulation does not pass UL94 test in vertical position. From the UL94 results alone, it is not possible to differentiate behaviour of flame retarded polymers because all these formulations are V0 rated. For the LOI measurements, PG4A has the highest LOI (35.5%), followed by PG3B (31.5%), PG2 (28%) and PG1 (19.5%). The fact that Alpi alone achieves a higher LOI than Alpi with Nano-MMT is somehow unexpected. This result highlights that although LOI measurement provides a numerical result convenient to rank materials, it does not correspond to an intrinsic material property and LOI value depends on experimental characteristics such as effective heat transfer coefficient to the sample for instance [8]. Clearly, the efficiency of the FR contained in the polymer in real scale fire conditions cannot be revealed by UL 94 vertical and LOI tests only. In comparison, the cone

calorimeter test provides much more realistic burning behaviours that are observed in real fire conditions and also a means to deduce the fundamental flammability properties of these materials.

Table 2. Results of limiting oxygen index and UL 94 tests.

	PG1	PG2	PG3B	PG4A
LOI (%)	19.5	28.0	31.5	35.5
UL-94 Vertical (nom 3.2mm)	Fail	V0 Pass	V0 Pass	V0 Pass

Experimental details

Tests were conducted at six heat fluxes, i.e. 22.5, 30, 45, 60, 75 and 90kW/m^2 in horizontal position and at 75kW/m^2 in vertical configuration. Each test is repeated two or three times. Time to ignition (TTI), heat release rate (HRR), mass loss rate (MLR) and production of carbon monoxide, carbon dioxide and smoke were recorded. The exposed surface of the plates is covered with carbon black. Before the tests, all samples were kept in a conditioning room maintained at an atmosphere of 50 ± 5% of relative humidity and at 23 ± 2˚C until their mass was stabilized. All the experiments were carried out with an insulation consisting of four layers of low-conductivity cotronic paper at the back of the specimen in order to reduce heat losses to the sample holder [9]. Aluminium foil is used to avoid melted polymer to soak in insulation paper.

Results and discussions

Visual observations

After the tests, sample residues present different visual aspects depending on both formulations and external heat fluxes. For the PG1and PG2 formulations, small pores due to glass fibres are visible at the surface of the residue and colour goes from white (high heat fluxes) to dark grey (below 30kW/m^2). These residues are mainly composed of glass fibres, as the weight of the residues is similar to the initial glass fibre content in these formulations. For PG3B and PG4A formulations, black residues are observed. For PG4A, this carbonaceous char is bumpy and porous whereas it is smoother and stiffer for PG3B. Observed carbonaceous chars for PG3B and PG4A are an indication of solid phase action of Alpi and Nano-MMT.

Time to ignition

Table 3 summarises the average ignition times for the tests in horizontal configuration. At heat fluxes lower than 45kW/m^2, flashes were often observed before a sustained combustion. The ignition behaviour of PG2 is different at these low heat fluxes: flashes were still observed but the sparkle igniter had to be maintained much longer when first flames appear in order to reach sustained combustion. This illustrates the gas phase action of the brominated polystyrene contained in PG2 samples. The measurement of the ignition times is consequently less accurate for PG2 as it is difficult to differentiate transitory flaming from sustained flaming.

Table 3: Averaged time to ignition (s) at different heat fluxes (kW/m^2)

Formulations	22.5kW/m^2	30kW/m^2	45kW/m^2	60kW/m^2	75kW/m^2	90kW/m^2
PG1	228	101	44.5	26	15	12.5
PG2	335	116	43	26	12	9.7
PG3B	329	158	55	32	14.5	11.2
PG4A	390	150	51.5	29	16	9.3

It can be seen from Table 3 that at the two lower heat fluxes, the action of flame retardants seems very efficient on delaying ignition. For PG2 and PG3B, an increase in the TTI of about 30% compared to PG1 is observed at 22.5kW/m^2 and 40% for PG4A. However, at higher heat fluxes PG2 has actually lower TTIs than PG1, indicating that the action of brominated polystyrene on TTI is less efficient than the one observed for Alpi or Alpi combined with Nano-MMT. Similar findings were reported in [10,11], which show that Alpi increases the TTIs of PBT-GF [10,11].

Determination of effective thermal properties

The average TTIs can be used to determine the effective thermal properties of the materials. For thermally thick conditions, theory and experiments have suggested that ignition usually occurs at a constant temperature, independent of the imposed heat flux, and that thermal properties can be determined from the unpyrolysed material by plotting the inverse square root of the ignition time versus the external heat flux [12]. However, if materials are thermally intermediate or thin, a modification of plotting ignition time data is required in order to correct thermal properties and the critical heat flux of the material [13]. The thermal diffusivity, α, is then adjusted to obtain the same intercept for both curves. This intercept corresponds to 64% of the critical heat flux. This critical heat flux is then used to find the ignition temperature with a energy balance at the surface of the material when no ignition occurs:

$$\dot{q}''_{cri} = \varepsilon\sigma\left(T_{ig}{}^4 - T_{amb}{}^4\right) + h_c\left(T_{ig} - T_{amb}\right) \tag{1}$$

For simplicity, the surface emissivity ε is assumed equal to 1 as the sample surface was painted with carbon-black. The convection heat transfer coefficient h_c is taken equal to 7W.m^{-1}.K^{-1} [14]. The density of the samples is determined based on the weight and volume. The specific heat of the material is finally found assuming that the inverse of the slope of thermally thick configuration is equal to:

$$\frac{\sqrt{\pi}}{2}(T_{ig} - T_0)\sqrt{k\rho c} \tag{2}$$

An illustration of this method is plotted in Fig. 1 for PG4A assuming a thermal diffusivity of 5.5x10^{-8}m^2/s. Results for all materials are listed in Table 4.

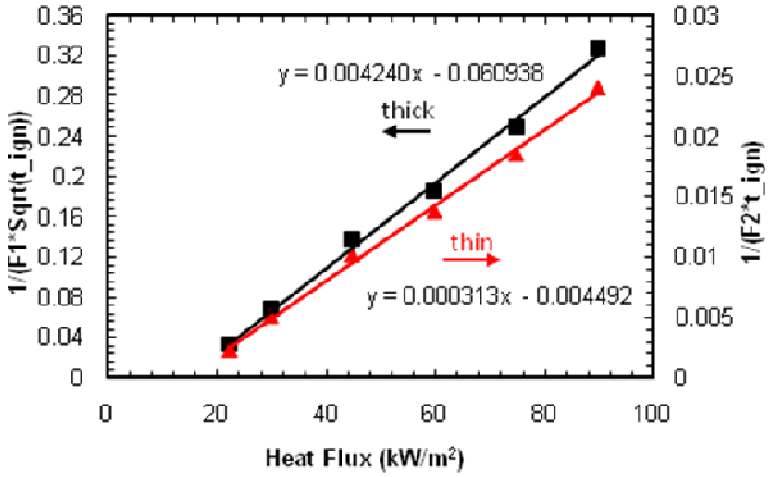

Figure 1. Corrected ignition times for PG4A (α=5.5x10^{-8}m^2/s).

Table 4. Thermal properties of PG1, PG2, PG3B and PG4A derived from the ignition data.

Formulation	ρ (kg/m^3)	α x10^8 (m^2/s)	$\dot{q}''_{cri}$ (kW/m^2)	T_{ig} (K)	k (W/m.K)	c (J/kg.K)	$k\rho c$ (kJ^2/m^4.K^2.s)
PG1	1520	4.9	12.2	647	0.17	2215	0.56
PG2	1610	5.8	18.4	725	0.14	1490	0.33
PG3B	1495	5.1	19.9	742	0.13	1770	0.36
PG4A	1490	5.5	22.5	767	0.12	1520	0.28

Table 4 clearly shows that when FRs are added there is an increase of the critical heat flux (the minimal heat flux for ignition) whereas a decrease of the thermal inertia, $k\rho c$. When a sample with low thermal inertia is exposed to the same heat flux, its surface temperature increases faster than that one with higher thermal inertia and thus it reaches its ignition temperature more quickly. PG2, PG3B and PG4A have approximately the same thermal inertia, which explains why the TTIs of the three materials are similar.

The thermal penetration depth, δ, is defined as $\delta = \sqrt{\alpha t_{ig}}$ where α is the thermal diffusivity of the solid and t_{ig} the time to ignition at a given heat flux. The thermal penetration depths are calculated for the four formulations at all heat flux and plotted in Fig. 2, which shows that for 22.5 and 30kW/m^2 heat fluxes, the samples are thermally thin or intermediate whereas they behave as thermally thick for higher heat fluxes.

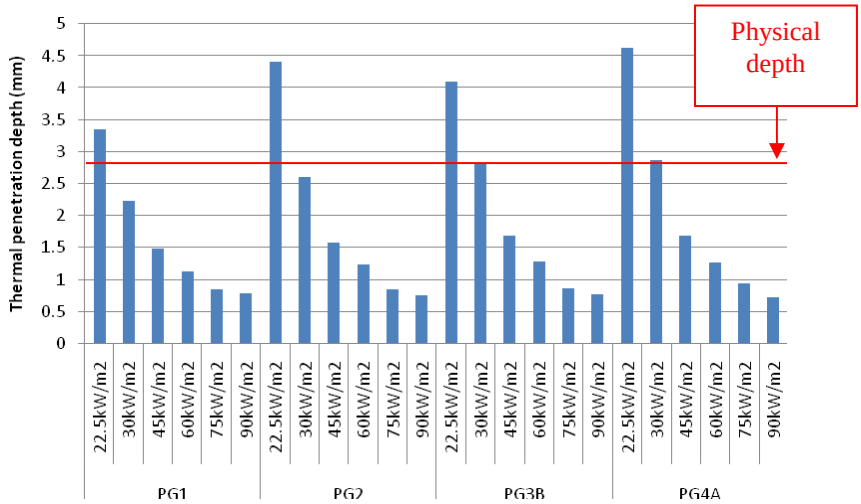

Figure 2. Thermal penetration depth of PG1, PG2, PG3B and PG4A formulations exposed to 22.5, 30, 45, 60, 75, 90kW/m^2 heat fluxes.

Mass loss rate

Figure 3 compares the mass loss rates of the four formulations at 45 and 60 kW/m^2. The shapes of mass loss rate are characteristic of charring material: the mass loss rate 1) increases to reach a first peak, 2) decreases rapidly to reach a plateau whose length depends on sample thickness and external heat flux, 3) increases again to form a second peak and 4) finally decreases when most of the fuel is burnt. The decrease of the mass loss rate after the first peak is the consequence of the formation of a surface shield by the accumulation of glass fibres [15]. It reduces the pyrolysis gas supply to the combustion zone by retarding the heat transfer from the surface material to the virgin zone. The second peak is to due to the backside effect. When the heat reaches the back surface, there is an accumulation of energy due to the insulation, which results in an increase of the mass loss rate.

The mass loss rates of PG1 and PG2 are very close and the first peak MLRs ranges from 0.2 and 0.33 g/s depending on the incident heat flux. This result indicates that that the brominated polystyrene does not act in the solid phase or, even if it does, its action is not significant.

For PG4A, a thin char layer is formed at the sample surface after ignition, which could be responsible for the reduction in the first peak MLR especially at higher heat flux (decrease of 30% at 75kW/m^2). However, no effect is observed on the second peak, which sometimes is even slightly higher than that of PG1. When Nano-MMT is added, the MLR is reduced further by between 30 and 50% depending on the external heat flux. However, the pyrolysis process is prolonged by around 40s at 75kW/m^2 to 110s at 30kW/m^2. The reduction of the mass loss rate and the prolongation of the pyrolysis process for PG3B are due to the formation of a char-like surface which absorbs some of the energy and reduces the backside effect.

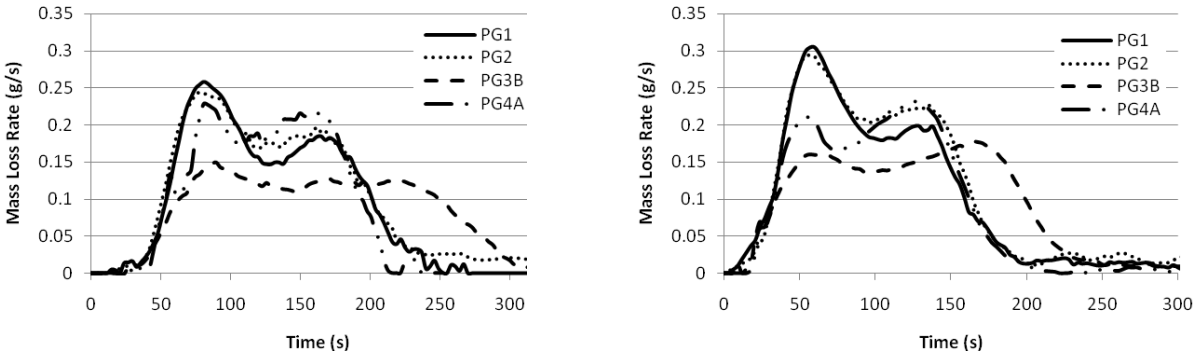

Figure 3. Comparison of mass loss rate (g/s) in cone calorimeter at 45kW/m^2 (left hand side) and 60kW/m^2 (right hand side) for PG1, PG2, PG3B and PG4A formulations.

Heat release rate

Figure 4 shows the heat release rates (normalised by the exposed surface area) of the four formulations at 45 and 60 kW/m^2. While the mass loss rates of PG1 and PG2 are similar (see Fig. 3), their heat release rates are very different. The brominated polystyrene reduces the heat release rate by more than 70% at higher heat fluxes, especially for the first peak. This indicates a strong gas phase action of the brominated FR, which basically consists in interacting with the highly reactive free-radical species such as H• and O• by slowing down or stopping the cascade-chain mechanism of the combustion [16]. PG2 produces the lowest HRR among all formulations at all heat fluxes.

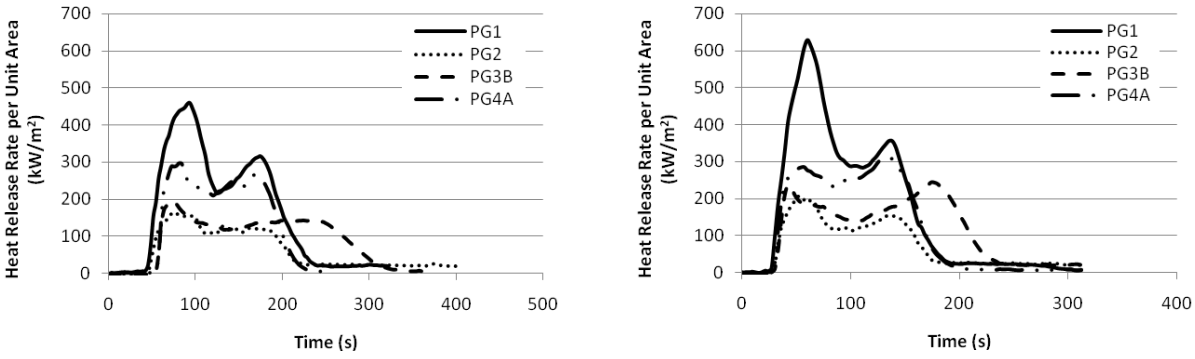

Figure 4. Comparison of heat release rate per unit area (kW/m^2) in cone calorimeter at 45kW/m^2 (left hand side) and 60kW/m^2 (right hand side) for PG1, PG2, PG3B and PG4A formulations.

For PG4A, it can be observed in Fig. 4 that at 60 kW/m^2 the MLR is only about 25% lower than PG1 at its first peak, and then becomes similar afterwards. The HRR of PA4A (see RHS of Fig. 3), on the other hand, shows a reduction of about 60% at its first peak and about 25% for the rest of the test. The different behaviours observed for the MLR and HRR between PG1 and PG4A illustrate a gas phase action of Alpi. The present results is consistent with that in [11], which showed a decrease in first peak of heat release rate of about 45% when 20% Alpi is used in PBT-GF and no difference in second peak and decrease of heat release rate.

For PG3B, there is a further reduction of the HRR compared to PG4A. The peak HRRs for PG3B is comparable with that for PG2, however with a prolonged burning process. The reduction of the HRRs by Nano-MMT is likely due to the improved char strength of Alpi in the presence of nanoparticles. It is the well-known action of Nano-MMT [17, 18] which decreases the mass loss rate and the heat release rate by forming a char-like surface due to the migration of the nanoclays to the surface of the pyrolysing sample. It is however worth noting that though a reduction in the transient HRR, Nano-MMT does not decrease the total heat release, indicating that the action of Nano-MMT is only physical.

Effective heat of combustion $\Delta H_{c,eff}$

The effective heat of combustion is defined as the product of the theoretical heat of combustion $\Delta H_{c,theory}$ with combustion efficiency χ, and can also be calculated using the total heat released (THR) divided by the total mass loss $|\Delta m|$ as:

$$\Delta H_{c,eff} = \chi \cdot \Delta H_{c,theory} = \frac{THR}{|\Delta m|} \tag{3}$$

The effective heat of combustion normalized by the mass PBT-GF contained in each formulation is plotted in Fig. 5. It is assumed that the proportion of PBT and FRs in the gaseous phase is the same as in the solid one. This assumption is correct for PG2 as most of the brominated polystyrene goes in gaseous phase. However, for PG3B and PG4A formulation, as Nano-MMT and a part of Alpi and PBT (about 20 wt. %) remains in the solid phase, it is expected that proportion of compounds in gaseous phase is slightly different. For PG4A and PG3B formulation, it induces an overestimation of values plotted in Fig. 5.

PG1 formulation has the highest effective heat of combustion with an average value of 15.5kJ/g. PG2 formulation shows the lowest effective heat of combustion for equivalent amount of PBT with values ranging from 5.6 to 8.8 kJ/g. It corresponds to a decrease of about 55% when compared to PG1 formulation. This decrease in effective heat of combustion of BrFR formulation illustrates the gas phase action of brominated polystyrene. Although the total mass loss for PG2 experiments is constant for all heat fluxes, the effective heat of combustion increases with the external heat flux. The efficiency of the gas phase action of brominated polystyrene seems to decrease with increasing heat flux. It is also illustrated by the difficulties to ignite PG2 samples described previously and local extinction at lowest heat fluxes. PG4A formulation shows a decrease of about 15% in the effective heat of combustion divided by the weight percentage of PBT-GF. As mentioned previously, this decrease is underestimated and Alpi in PBT-GF therefore shows an action in gaseous phase. PG3B formulation has equivalent effective heat of combustion to PG4A although PG3B burning process lasts longer with lower mass loss rate. Nano-MMT reduces the maximum heat release rate but does not change the total amount of heat released.

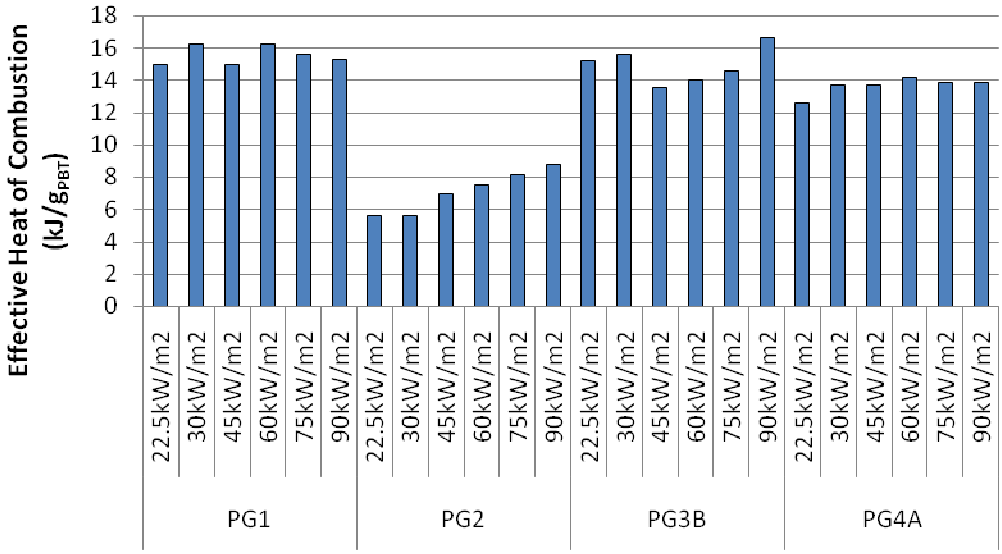

Figure 5. Comparison of effective heat of combustion (kJ/g_{PBT}).

Effective heat of combustion of 22kJ/g [19] was reported for pure PBT and 21kJ/g for PBT-GF [11]. A lower value of 15.5kJ/g is measured for PG1 in our experiments. Such discrepancy could be due to the difference in the PBT samples. Unfortunately, no pure PBT samples were available for this work to support this claim.

Production of smoke, carbon monoxide and carbon dioxide

Carbon monoxide, carbon dioxide and smoke yields are calculated from the pre-ignition period until the flame goes out. The smoke production rate is calculated as the volume flow rate in the exhaust duct times the extinction coefficient. Results are plotted in Figs. 6 to 9.

PG1 has the lowest CO and smoke yields and production rates but highest CO_2 yield and production rate. It illustrates a more complete combustion than the three other formulations. The combustion of PG2 yields about 20% more smoke than other FR formulations and 55% more than PG1. Its peak values of smoke production rates are 2.5 times higher than those obtained for PG1. PG4A yields more than 15% of CO than PG2 and almost 80% more than PG1. CO is produced 15% more by PG4A than by PG2. It is generally considered that an increase in smoke and CO production by a factor of more than two is the consequence of a suppressed total oxidation process and is synonym of a radical trapping mechanism. Consequently brominated polystyrene and Alpi may act in the gas phase as radical scavengers. When Nano-MMT is combined with Alpi in PG3B, the same amount of CO, CO_2 and smoke is produced than when Alpi is used alone. However, the use of Nano-MMT reduces the rate at which these species are released by 45% 30% and 25% for CO, CO_2 and smoke respectively.

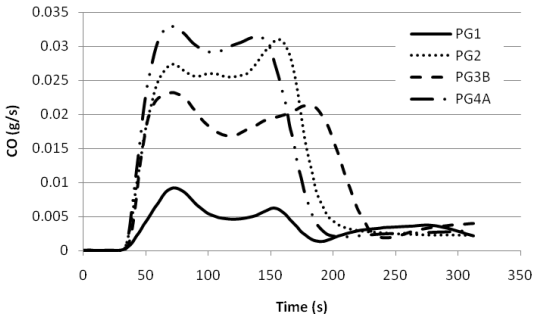

Figure 6. CO production rate (g/s) at 60kW/m^2 in horizontal cone calorimeter.

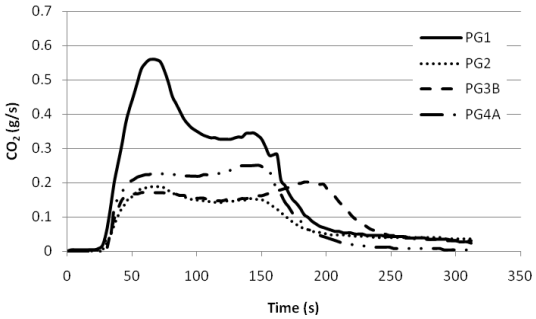

Figure 7. CO_2 production rate (g/s) at 60kW/m^2 in horizontal cone calorimeter.

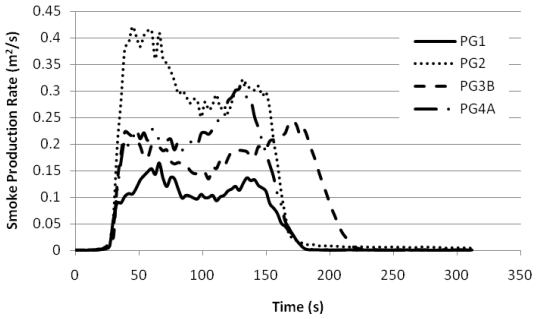

Figure 8. Smoke production rate (m^2/s) at 60kW/m^2 in horizontal cone calorimeter.

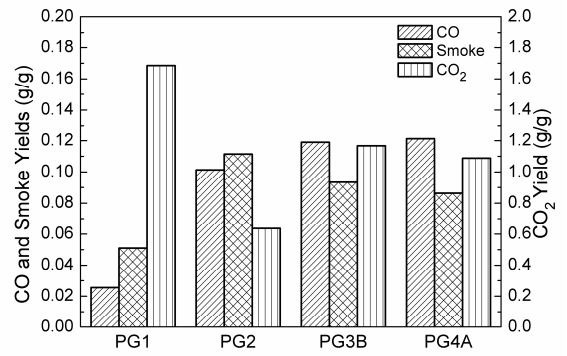

Figure 9. Average CO, CO_2 and smoke yields (g/g) for investigated PBT/GF samples in cone calorimeter at six heat fluxes.

Backside temperature of sample

The temperature of the back of the sample was measured by placing a type K thermocouple with bead size of 0.5mm between the sample and the insulation. The temperature histories at 60kW/m^2 are plotted in Fig. 10. About 20 seconds after ignition occurs, a sharp increase of the backside temperature is observed for PG1, PG2 and PG4A. This transition corresponds to the time needed for the heat to be conducted to the back of the sample. The increase in temperature for PG3B is not as sharp as for other formulations. This is consistent with previous observations that lower HRR and MLR were found for PG3B, owing to the improved char strength by Nano-MMT, which prevents heating transferring to the back surface.

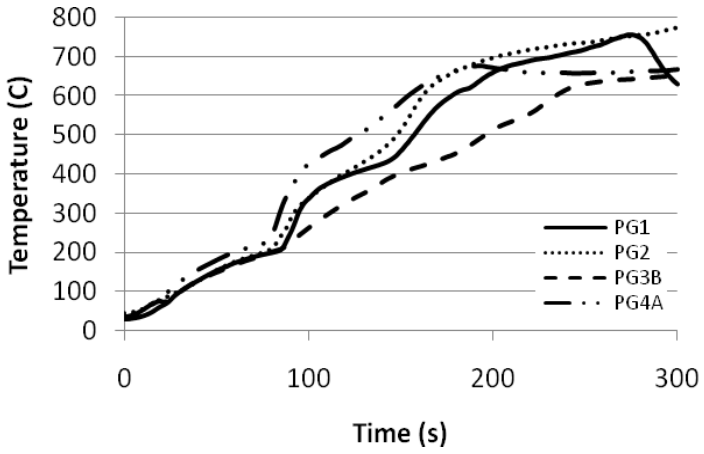

Figure 10. Comparison of backside temperature during cone calorimeter tests at 60kW/m^2.

Cone calorimeter tests in vertical position

Cone calorimeter tests in vertical orientations are mostly conducted for charring materials to assess the strength of the char, because non-charring materials such as thermoplastics will whether melt and spill out of the trough of sample holder or bend out of shape and separate from the sample holder. If the char is strong enough, the sample will stay in position and no excessive melt or spill out will be observed. Because the char formed by Alpi in PG3B and PG4A and that by glass fibre are strong enough, it was possible to conduct cone calorimeter measurements to assess the action of FRs in different orientations.

For PG1, it was observed that the base of the flame is located in the trough, which indicates that a part of the base polymer melts and burns from that trough. However, neither excessive dripping behaviour nor spilling over the rig was observed for all formulations. Figures 11 to 14 show the mass loss and heat release rates at 75kW/m^2 in both horizontal and vertical orientations. Both mass loss and heat release rates are about 30% lower in vertical orientation than in horizontal orientation. This difference is mainly due to different convective heat transfer coefficient and flame radiation to the sample. The action of brominated polystyrene and Alpi is however similar for both orientations.

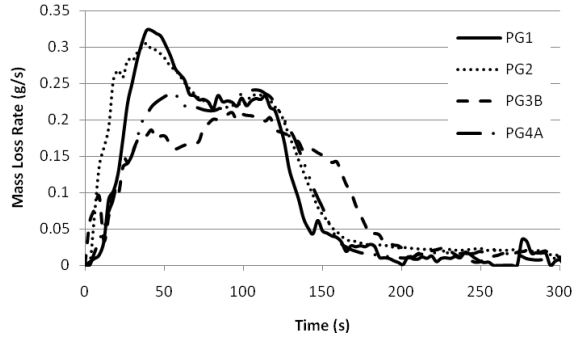

Figure 11. Mass loss rate (g/s) in horizontal position at 75kW/m^2.

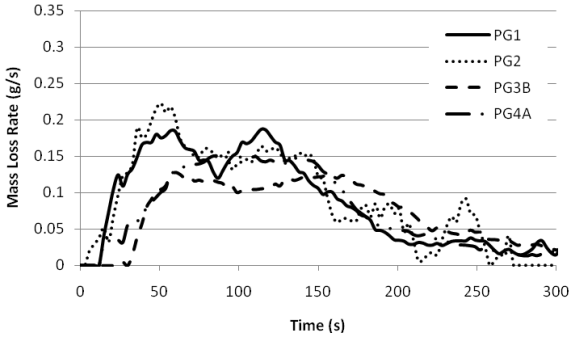

Figure 12. Mass loss rate (g/s) in vertical position at 75kW/m^2.

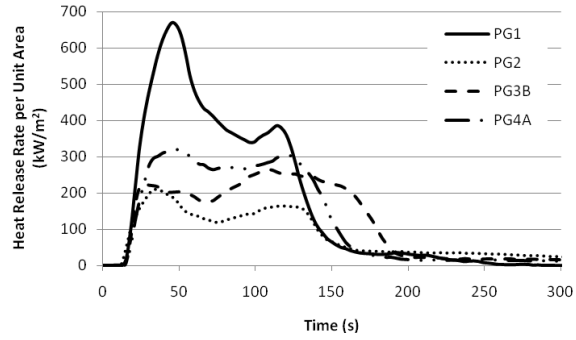

Figure 13. Heat release rate per unit area (kW/m^2) in horizontal position at 75kW/m^2.

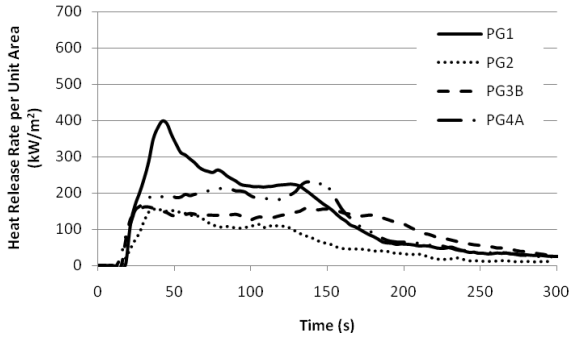

Figure 14. Heat release rate per unit area (kW/m^2) in vertical position at 75kW/m^2.

Conclusions

Glass fibre reinforced PBT was modified with a halogenated fire retardant (HFR), brominated polystyrene combined with antimony trioxide, and two halogen free fire retardants (HFFRs), Alpi with/without Nano-MMT. The fire retardancy of these materials was assessed in LOI, UL94 and cone calorimeter. The major conclusions of this work are:

1) All formulations exhibit charring burning behaviour with two peaks in the mass loss and heat release rates due to the shielding action of the residue consisting of glass fibres and char with/without nanoparticles.

2) Key flammability parameters such as time to ignition, heat release rate, efficiency of combustion and smoke and carbon monoxide yields were measured in cone calorimeter at six heat fluxes and used to compare the fire behaviour of formulations and obtain some material flammability properties.
3)
    a. The brominated polystyrene has no action in the solid phase (Fig. 3) but bromine released in the pyrolysis reduces the effective heat of combustion by about 55% (Fig. 2). However it also produces CO and smoke at excessive rates compared to the base formulation (PGT+GF30%) (Figs. 6 to 9);
    b. Alpi (PG4A) acts both in the condensed phase by modifying the char residue (Fig. 3) and in gaseous phase by decreasing the effective heat of combustion (Fig. 2). However the major effect is in the solid phase. The use of Alpi increases the ignition time (Table 3), provides the highest LOI of all formulations (Table 2) and decreases the peak of heat release rates (Fig. 4). Although the Alpi formulation produces less smoke than the brominated one (PG2), it releases more CO than PG2 (Figs 6 and 9);
    c. When Nano-MMT is combined with Alpi (PG3B), the LOI is lower than when Alpi is used alone but it is still higher than PG2 (Table 2). In the cone calorimeter, this combination, PG3B, provides better fire performance than PG4A with higher reduction of mass and heat release rates (Figs. 4, 13 & 14). CO and smoke yields of PG3B and PG4A are comparable (Fig. 9). The combination of Alpi and Nano-MMT in PG3B appears to be the best alternative to the brominated FR in PBT-GF. The decrease in mass loss rate of PG3B is due to the improved consistency of the residue (glass fibre, nanoparticles and char) produced by Alpi in the presence of Nano-MMT whereas the reduction in the HRR is due directly to the reduction in the MLR because the measured heat of combustion is close to the heat of combustion of the base formulation
4) Burning behaviour in horizontal or vertical orientations is similar except that lower HRRs are measured in vertical orientation owing to reduced flame heat fluxes compared to the burning in horizontal orientation. No dripping was observed in vertical orientation for all formulations.
5) The present study also highlights the limitations of LOI and UL94 measurements. UL94 test cannot differentiate materials with the same rating (V0 in this case). The LOI results in this work indicate that the formulation containing only Alpi (PG4A) has the lowest LOI. However, the cone calorimeter results clearly showed that PG2 and PG3B have similar HRRs, which are much lower than those of PG4A. In addition, LOI and UL94 tests cannot take into account smoke and CO production, which are important hazards in fires.

References

[1] Hites, RA., “Polybrominated diphenyl ethers in the environment and in people: a meta-analysis of concentrations”, Environ. Sci. Technol. 38: 945-956 (2004)

[2] Fängström, B., Strid, A., Grandjean, P., Weihe, P., Bergman A., “A retrospective study of PBDEs and PCBs in human milk from the Faroe Islands”, Environ. Health 4: 12 (2005)

[3] Schecter, A., Päpke, O., Tung, K., Joseph, J., Harris, T., Dahlgren, J., “Polybrominated diphenyl ether flame retardants in the U.S. population: current levels, temporal trends, and comparison with dioxins, dibenzofurans, and polychlorinated biphenyls”, J. Occup. Environ. Med. 47: 199-211 (2005)

[4] She, J., Holden, A., Sharp, M., Tanner, M., Williams-Derry, C., Hooper, K., "Polybrominated diphenyl ethers (PBDEs) and polychlorinated biphenyls (PCBs) in breast milk from the Pacific Northwest", Chemosphere 67: S307-317 (2007)
[5] Schantz, S., Widholm, J., Rice, D., "Effects of PCB exposure on neuropsychological function in children" Environ. Health Perspect. 111: 357-576 (2003)
[6] Stapleton, H., Dodder, N., Offenberg, J., Schantz, M., Wise, S., "Polybrominated Diphenyl Ethers in house dust and clothes dryer lint" Environmental Sci Technol. 38 (2004)
[7] Dingemans, M., Ramakers, G., Gardoni, F., Van Kleef, R., Bergman, A., Di Luca, M., Van den Berg, M., Westerink, R., Vijverberg, H., "Neonatal exposure to brominated flame retardant BDE-47 reduces long-term potentiation and postsynpatic protein levels in mouse hippocampus", Environ. Health Perspect, 115: 865-870 (2008)
[8] Suzanne, M., Delichatsios, M., Zhang, J., "Prediction of the limiting oxygen index using simple flame extinction theory and material properties obtained from bench scale measurements", Proc. of 10th IAFSS.
[9] de Ris, J., Khan, M., "A sample holder for determining material properties", Fire and Materials, 24: 219-226 (2000)
[10] Braun, U., Schartel, B., "Flame retardancy mechanisms of aluminium phosphinate in combination with melamine cyanurate in glass-fibre-reinforced Poly(1,4-butylene terephthalate)", Macromolecular materials and engineering, 293: 206-217 (2008)
[11] Braun, U., Bahr, H., Sturm, H., Schartel, B., "Flame retardancy mechanisms of metal phosphinates and metal phosphinates in combination with melamine cyanurate in glass-fber reinforced poly(1,4-butylene terephtalate): the influence of metal cation", Polymers for advanced technologies 19: 680-692 (2008)
[12] Delichatsios, M., "Ignition times for thermally thick and intermediate conditions in flat and cylindrical geometries", Proc 6th IAFSS, pp 233–244
[13] Delichatsios, M., "Piloted ignition times, critical heat fluxes and mass loss rates at reduced oxygen atmospheres", Fire Safety J. 40: 197-212 (2005)
[14] Zhang, J., Delichatsios, M., "Determination of the convective heat transfer coefficient in three-dimensional inverse heat conduction problems", Fire Safety J. 44: 681-690 (2009)
[15] Casu, A., Camino, G., De Giorgi, M., Flath, D., Laudi, A, Mornone, V., "Effect of glass fibres and fire retardant on the combustion behaviour of composites, glass fibres-poly(butylene terephthalate)", Fire and Materials 22: 7-14 (1998)
[16] Lewin, M., Weil, E., Fire Retardant Materials, Woodhead Publishing Ltd, 2001.
[17] Zhang, J., Delichatsios, M., "Further Validation of a Numerical Model for Prediction of Pyrolysis of Polymer Nanocomposites in the Cone Calorimeter", Fire Technology 46: 307–319 (2010)
[18] Zhang, J., Hereid, M., Hagen, M., Bakirtzis, D., Delichatsios, M., Fina, A., Castrovinci, A., Camino, G., Samyn, F., Bourbigot, S., "Effects of nanoclay and fire retardants on fire retardancy of a polymer blend of EVA and LDPE", Fire Safety J. 44: 504-513 (2008)
[19] Brehme, S., Schartel, B., Goebbels, J., Fischer, O., Pospiech, D., Bykov, Y., Döring, "Phosphorus polyester versus aluminium phosphinate in poly(butylene terephthalate) (PBT): Flame retardancy performance and mechanisms", Polymer Degradation and Stability 96: 875-884 (2011)